Journal of Thermal Engineering, Vol. 4, No. 3, pp. 1912-1925, April, 2018
Yildiz Technical University Press, Istanbul, Turkey

A NUMERICAL STUDY OF FORCED CONVECTIVE FLOW IN MICROCHANNELS HEAT SINKS WITH PERIODIC EXPANSION-CONSTRICTION CROSS SECTION

A. Belhadj[1,*], R. Bouchenafa[2] , R. Saim[2]

ABSTRACT

This paper aims to study numerically the laminar convective heat transfer of ionized water flow inside rectangular heat sinks with periodic expansion-constriction cross-section; each heat sink consists of parallel microchannels system with 4 mm wide and 0.1 mm deep in constant cross-section segment. Two-dimensional laminar numerical simulations, based on Navier-Stoks equations and energy equation, are obtained under the same boundary conditions for different microchannels. In this study, the heat transfer and pressure drop inside microchannels with cross-section (cylindrical grooves and triangular cavities) are compared with that of simple smooth microchannel at Reynolds number ranging from 150-1500; an increase in pressure drop of 44% for all microchannels is observed with Reynolds number increasing. The obtained results indicate an enhancement in Nusselt number for all microchannels at all Reynolds number values with a maximum enhancement of 36%, these ameliorated thermal parameters attribute to enhance the heat transfer efficiency of proposed microchannels. Which improve the effect of periodic expansion-constriction cross-section on the heat transfer performance for microelectromechanical systems (MEMS) cooling phenomena.

Keywords: *Cooling Systems, Heat Transfer Enhancement, Heat Sink, Microchannels, MEMS, Cross Section*

INTRODUCTION

Because of the miniaturization of the recent industrial systems, Micro-Electro Mechanical systems (MEMS), [1] are used to solve the problem of heat evacuation for electronic devices, to maintain their temperatures in a safe range in order to ensure their performance. Micro-technology has ensured the fabrication of MEMS since thirty years ago. Nowadays, the micro-devices are widely used in electronic applications, especially for cooling the computer chips. Tuckerman and Pease [2] were the first persons who examined the earliest work on microchannel heat sink, they showed that microchannel heat sink gave a good heat dissipation rate from the electronic chips, and this result guaranteed the potential of this technology. In order to calculate heat transfer, Samalam [3] studied analytically and numerically a forced convective flow in microchannel for electronic devices cooling, he showed the optimum dimensions for width and microchannel spacing. After using the optimum values, microchannel heat sink had lower thermal resistance than original model. Peng et al [4, 5, 6] investigated the single-phase forced convective heat transfer of water in rectangular channels with hydraulic diameter ranging from 133 to 367 μm. Their results indicated that the Reynolds number for transition from laminar to turbulent flow became much smaller than in the macroscale channels, and the aspect ratio of the channel had a significant effect on the convective heat transfer. Margot et al.[7] has elaborated a numerical modelling of cavitation implemented in CFD code to investigate the three dimensional flow within Diesel injectors, they found that cavitation model was able to predict the onset of cavitation, they also find that in both the injection rate and the occurrence of chocked flow are satisfactory agreement when compared with experiments.

Sheikholeslami et al. investigated the forced convective flow under the influence of magnetic field in a semi annulus using variable magnetic field [8], using Fe3O4-water nanofluid with non-uniform magnetic field [9]. In addition, variable magnetic field using two-phase model [10], their results show that the Nusselt number has a direct relationship with the Reynolds number while it has a reverse relationship with the Hartmann number and Lewis number.

Farhanieh et al. [11] performed numerical and experimental studies on laminar fluid flow and heat transfer characteristics in a duct with a rectangular grooved wall. The results indicated an enhancement in the local Nusselt number compared to a smooth parallel plate duct due to reestablishment of thermal boundary layers and formation

This paper was recommended for publication in revised form by Regional Editor Jaap Hoffman Hoffman
[1]MECACOMP Laboratory, Department of Mechanical Engineering, Tlemcen University, Tlemcen, Algeria
[2] ETAP Laboratory, Department of Mechanical Engineering, Tlemcen University, Tlemcen, Algeria
**E-mail address: belhabdelkadir@gmail.com*
Manuscript Received 14 November 2016, Accepted 8 January 2017

of recirculation flows inside the grooves. They also showed a relatively high-pressure drop increase accompanying this enhancement. Qu and Mudawar [12] investigated numerically three-dimensional heat transfer in the silicon microchannel heat sink using the finite difference method. They concluded that the increasing Reynolds number increased the length of the developing region. Fully developed flow might not be achieved inside the heat sink for high Reynolds numbers. The results clearly showed that heat transfer performance is improved and the pressure drop becomes higher. Chai et al [13] studied the pressure drop and heat transfer characteristics of the interrupted microchannel heat sink with rectangular ribs in the transverse micro chambers, and analyzed the effects of dimension and position parameters of rectangular rib on these characteristics. Weilin et al [14] studied the flow in trapezoidal microchannels whose hydraulic diameters are between 51 and 169 μm, and showed a significant difference between the experimental results and theory. They then propose a behavioral model roughness/viscosity to interpret these differences. The effects of geometrical configuration such as aspect ratio, waviness and expansion factor on heat transfer performance and fluid flow of converging–diverging microchannels are studied numerically by Ghaedamini [15]. In the same context, Joshi et al. [16] studied the effect of wave amplitude, wavelength and aspect ratio for a Reynolds number ranging from 50 to 150. The zigzag shape channels with circular cross sections studied and compared to straight microchannels, by Zheng et al. [17]. Due to the presence of chaotic advection, the heat transfer was enhanced. Using the CFD (computational fluid dynamics) and LB (lattice Botlzmann) approaches, Liu et al. [18] numerically studied the heat transfer performance of microchannels with different surface microstructures. Xia et al. [19, 20] were studied the forced convection in microchannels with aligned fan-shaped reentrant cavities; they showed the effect of structural parameters on the fluid flow and conjugate heat.

Recently, Chai et al. [21] studied the heat transfer enhancement in microchannel heat sinks with periodic expansion–constriction cross-sections; they discussed the influences of periodic expansion–constriction cross sections on pressure drop, heat transfer and thermal resistance. Gururatana [22] numerically studied forced convective flow in microchannel heat sink with dimples, he showed the effect of dimples on heat transfer enhancement, by increasing average Nusselt number, and he concluded that dimples are useful when Reynolds number is greater than 125. Dehghan et al.[23] studied the laminar constrained fluid flow and conjugate heat transfer in microchannel heat sink with converging channels, they showed that the poiseuille number increases with increased tapering, while the required pumping power decreases, and the Nusselt number increases with tapering as well as the convection heat transfer coefficient.

In the present study, we present a numerical simulation of water flowing in two different microchannels fitted with periodic expansion-constriction cross-section. The performances of two microchannels are compared with parallel plates microchannel.

GEOMETRY AND BOUNDARY CONDITIONS

In this work, we are going to study for Two-Dimensional baseline case the forced convective heat transfer in three microchannels. Hence, the typical computational domain is illustrated in the figure 1; the rectangular ship is considered as microchannel with length of 4mm and width of 0.2mm. Two microchannels with periodic expansion-constriction cross-section are studied. The figure 1 shows the dimensions of the expansion– constriction cross-section. For the microchannel with cylindrical grooves (K), the radius is 0.1 mm, whereas for the microchannel with triangular reentrant cavities (L), the length of expansion cross-section is 0.06 mm and the length of the constriction cross-section is 0.14 mm in the direction of the flow, and the depth of the triangular reentrant cavity is 0.1 mm.

The boundary conditions for microchannel heat sink are shown in the figure 2. The upper, lower and additive cavities are defined as wall with non-slip condition. The velocity inlet and pressure outlet conditions are used on region AD and BC, respectively. Uniform velocity of 3 m.s-1 is employed for the flow inlet in the x direction. For heat transfer boundary condition, the constant temperature of 350 K is defined on lower and added sections surface, and the upstream bulk temperature of inlet flow is set to 300 K. The same temperature is defined at upper wall.

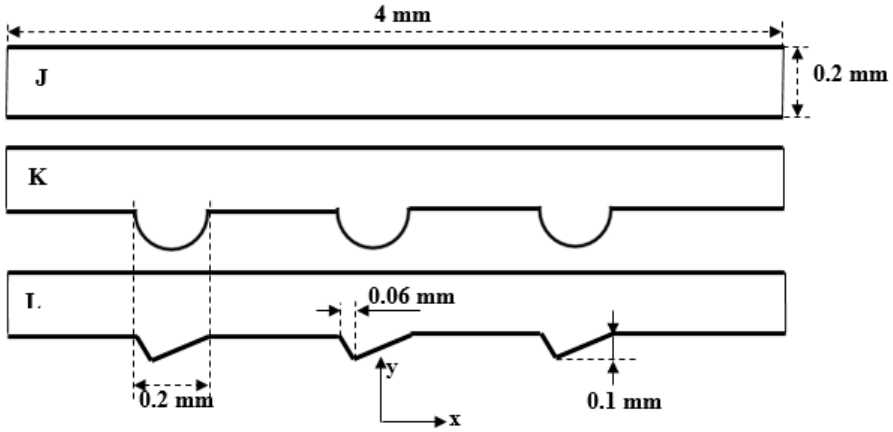

Figure 1. 2D microchannels heat sink

The isothermal boundary condition defined on the lower wall is due to the temperature of the electronic element to be cooled which is glued under the microchannel heat sink.in other case the appropriate boundary condition is a constant heat flux.

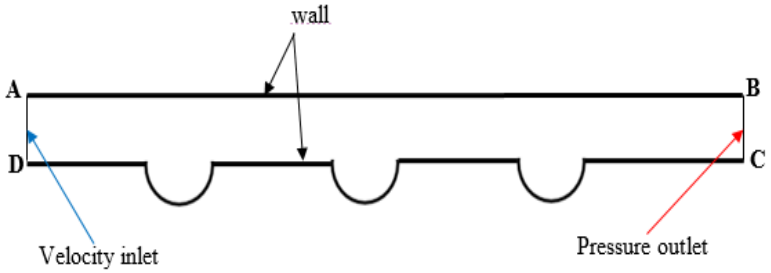

Figure 2. Boundary conditions for microchannels heat sinks.

GOVERNING EQUATIONS AND NUMERICAL METHOD

The Navies–Stokes and energy equations are used to model the convective heat transfer process with the following assumptions: Two-dimensional, incompressible, laminar and steady state. The effect of gravity and other forms of body forces are negligible. The properties can be considered as constant because of the narrow temperature range.

The continuity, momentum and energy equations for laminar flow [15] can be listed as Eq. 1-4:

$$\rho\left(\frac{\partial u}{\partial x}+\frac{\partial v}{\partial y}\right)=0 \tag{1}$$

$$\rho\left(u\frac{\partial u}{\partial x}+v\frac{\partial u}{\partial y}\right)=-\frac{\partial P}{\partial x}+\mu\left(\frac{\partial u^2}{\partial x^2}+\frac{\partial u^2}{\partial y^2}\right) \tag{2}$$

$$\rho\left(u\frac{\partial v}{\partial x}+v\frac{\partial v}{\partial y}\right)=-\frac{\partial P}{\partial y}+\mu\left(\frac{\partial v^2}{\partial x^2}+\frac{\partial v^2}{\partial y^2}\right) \tag{3}$$

$$\rho C_P\left(u\frac{\partial T}{\partial x}+v\frac{\partial T}{\partial y}\right)=\lambda\left(\frac{\partial T^2}{\partial x^2}+\frac{\partial T^2}{\partial y^2}\right) \tag{4}$$

Where, u and v are the velocity in streamwise and spanwise direction. P and T are the pressure and temperature. The ρ, Cp, λ and μ, which are the fluid properties, are density, specific heat, thermal conductivity and

dynamics viscosity, respectively. The commercial software package, Fluent 6.3.26, is used in this study. The governing equations are discretized by the finite volume method and the second order upwind scheme is adopted for spatial discretization of the convection terms. The segregated solver is used in the simulation and the SIMPLE algorithm is employed to couple the pressure and velocity (Patankar [24]). The convergence criteria of iterative solution have been insured when the residual of all variables are less than specific values. The specified value is $10^{-4}$for continuity, momentum and energy equations.

- ***Characteristic parameters***

The expression of friction coefficient is defined as follows:

$$f = \frac{2.\Delta P.D_h}{\rho {U_i}^2 L} \tag{5}$$

The flow Reynolds number is calculated as:

$$Re = \frac{\rho\, U_i D_h}{\mu} \tag{6}$$

The local Nusselt number can be written as:

$$Nu = \frac{h.D_h}{\lambda} \tag{7}$$

We can also obtain the average Nusselt number by:

$$\overline{Nu} = \frac{h_m D_h}{\lambda} \tag{8}$$

The heat transfer rate is defined as:

$$Q = m.C_p\left(T_f - T_i\right) \tag{9}$$

To compare between the studied microchannels, we define the heat transfer efficiencyas:

$$HTE = \frac{\left({Q_{mic}}/{Q_J}\right)}{\left({\Delta P_{mic}}/{\Delta P_J}\right)^{1/3}} \tag{10}$$

GRID EFFECT STUDY AND CODE VALIDATION

For an inlet velocity equal to 3 m/s, many meshing sizes have been tested to ensure the grid independence of results. Table.1 shows the various grids used for a Reynolds number equal to 500. The various values of axial velocities as well as the maximum value of the stream function and the average Nusselt number are presented. The values in the table indicate the properties at x = 2.5mm. The different meshing sizes indicate a difference in Reynolds number of 1.7 % at the same position. The mesh size of (9264nodes) as it is the smaller one giving accurate results has been chosen to model accurately the fluid flow in this problem and for further study (Table.1).

The variation of local Nusselt number along the lower (hot) wall is illustrated in Figure.3 to study the mesh refinement. It showed that the local Nusselt number converges for all values of nodes.

Table 1. Dependence of the properties on the meshing size (X = 2.5mm)

	8574 nodes	**9162 nodes**	**9264 nodes**	**9488 nodes**	**9578 nodes**
Ψ	0.0003698	0.0003698	0.000355	0.000355	0.000355
T_{min} (K)	299.999	299.999	299.999	299.999	299.999
U_{max} (m/s)	4.31091	4.33569	4.28902	4.25698	4.17556
Nu	24.7434	24.7622	24.8034	24.8287	24.8365
Time (s)	8.07	8.071	8.07	8.07	8.07

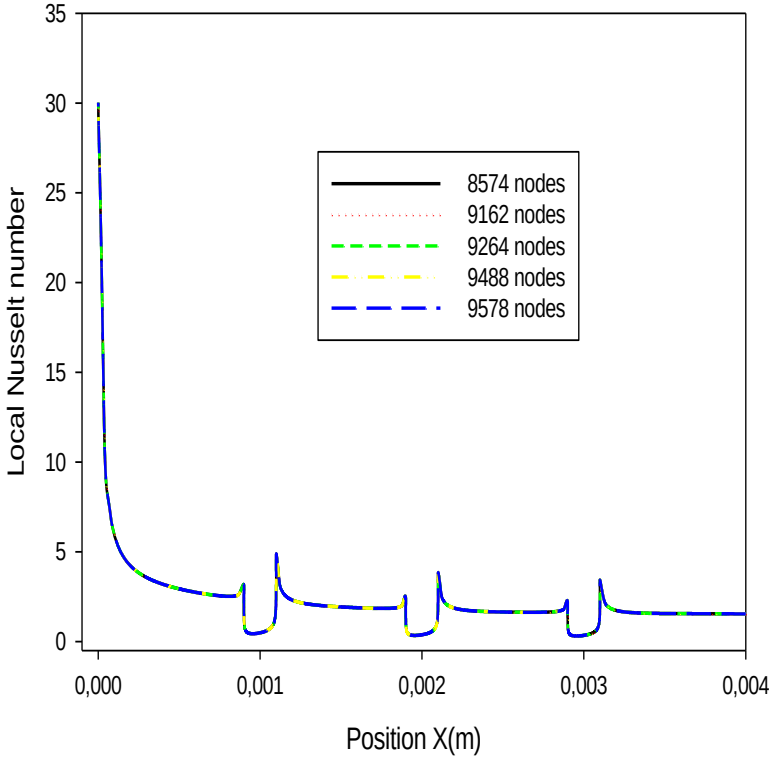

Figure 3. Influence of the mesh on the local Nusselt number

It is noticed that our study has no similar experimental work in literature particularly for laminar flow. That is why we will validate our numerical study using the empirical formula of Grigulland Tratz [25], who has numerically investigated the thermal entrance problem for laminar flow with constant heat flux. They evaluated the Nusselt number as a function of the dimensionless axial distance, Reynolds number, and Prandtl number.

$$Nu = 4.36 + \frac{0.00668\left(\frac{D_h}{X}\right)Re.Pr}{1+0.04\left[\left(\frac{D_h}{X}\right)Re.Pr\right]^{2/3}} \quad (11)$$

The figure 4 is plotted to make a validation for our numerical results, it showed that our numerical results converge with those obtained by Grigull Tratz formula, the local Nusselt number decrease with the length of microchannel for the steady flow.

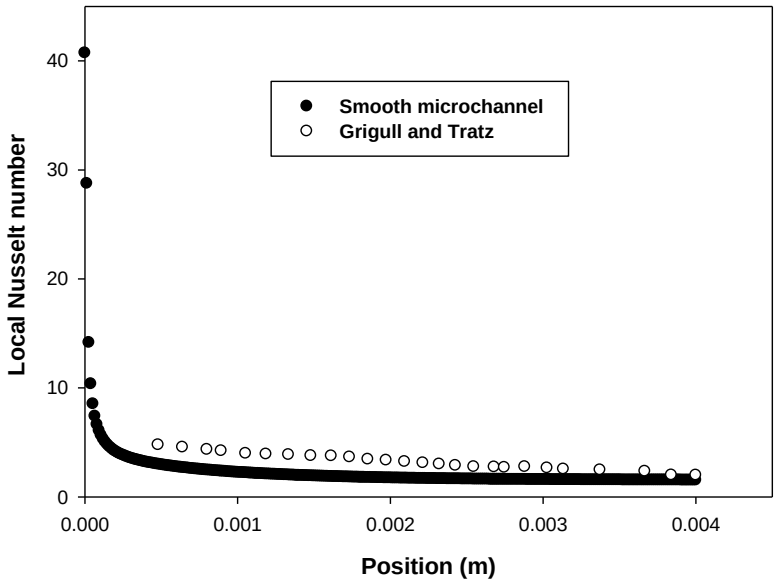

Figure 4. Comparison between calculated Local Nusselt number and that obtained using Grigull and Tratz formula.

RESULTS AND DISCUSSIONS

The study is focused on influence of the implementation of cylindrical grooves and triangle cavities on the dynamic and thermal behavior of the system for lower Reynolds number. Velocity profiles, friction factors, Nusselt numbers and isotherms are presented in two separate parts as hydrodynamics and heat transfer. For the presentation of the figures, Re = 500 is chosen as base case.

Hydrodynamic aspect

The figure 5. presents the longitudinal velocity distribution in three microchannels at Re=500 which corresponds an inlet velocity 3 m/s. It is found that the flow velocity of the medium reaches its maximum value (4m / s), and it is canceled near of the walls. In added sections, it showed a stagnation of velocity because of the high velocity applied in entry.

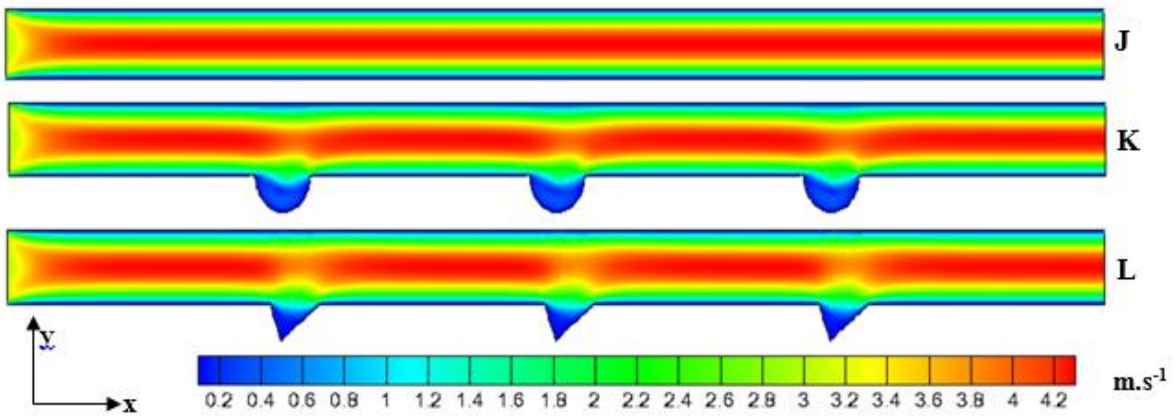

Figure 5. Contour of streamlines in the microchannels at Re=500.

The axial velocity profiles are studied in the figure .6 at position x=2.1mm from the entrance, exactly on downstream of the first expansion-constriction cross-section, it showed that the curves are different, which is explained by the effect of added sections on flow field. For the microchannel (K) the longitudinal velocity is non-zero on the lower wall because of the recirculation of the flow around the cylindrical groove shown in the Figure 8.

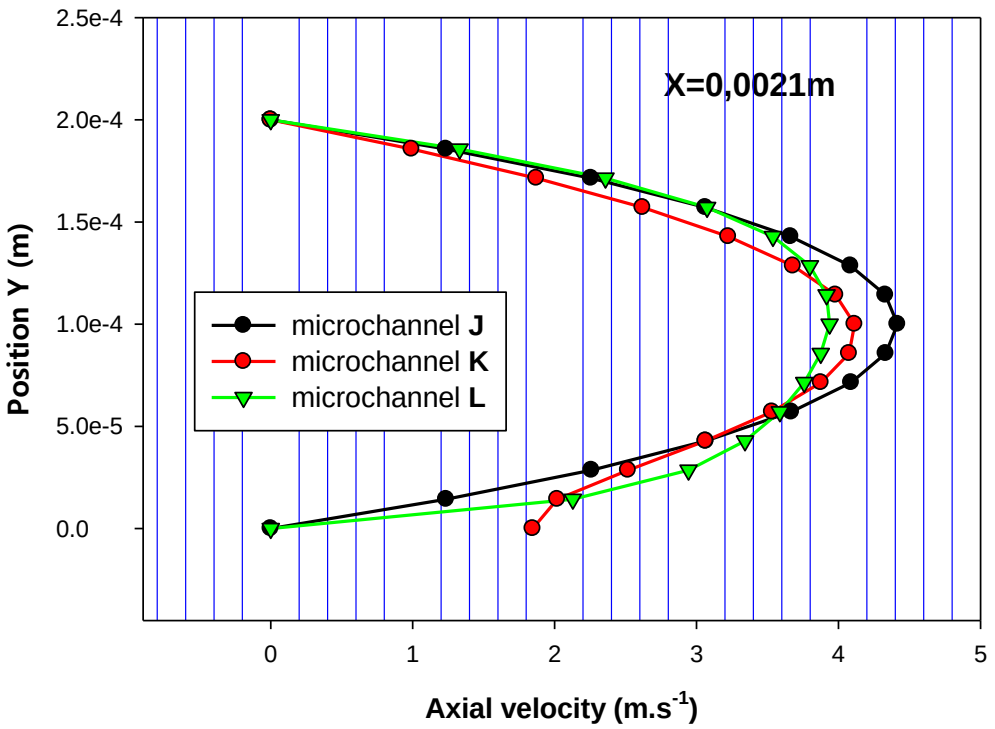

Figure 6. Axial velocity profiles at x=2.1mm

The figure 7 presents the axial velocity profiles far from the added sections at the positions x = 2.5mm. Curves are parabolic which improve the stability of flow field, for the microchannel (K) with cylindrical grooves, the axial velocity decrease over every cylindrical grooves.

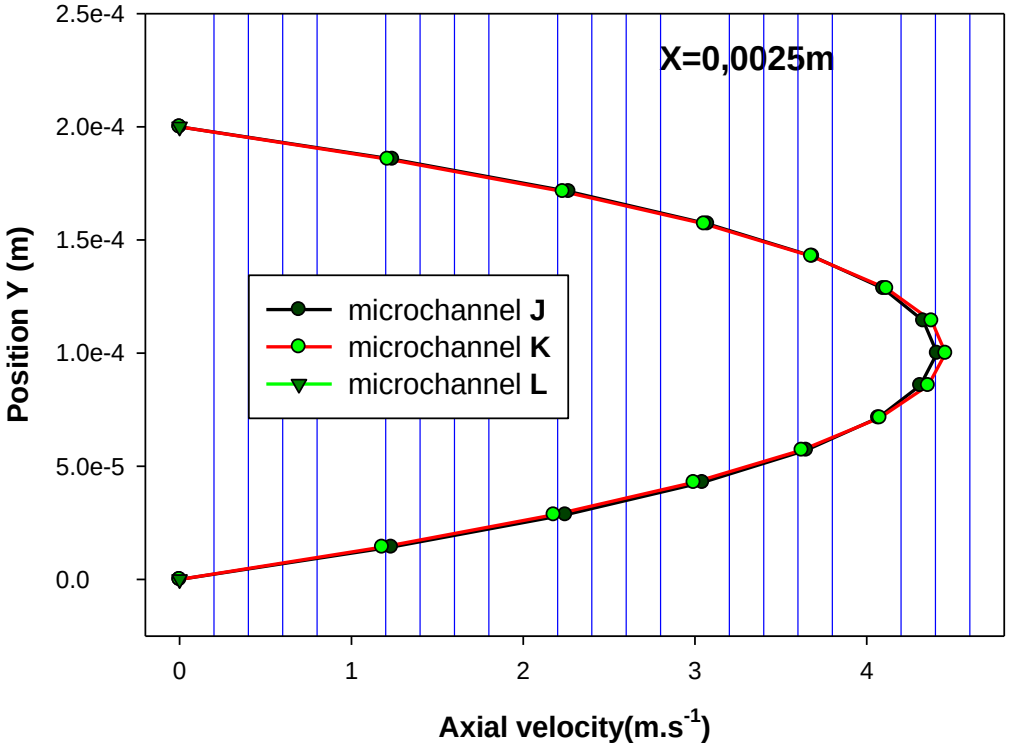

Figure 7. Axial velocity profiles at x=2.5mm

The figure 8 illustrates the velocity vectors over the cylindrical grooves, it shows a recirculation in the upstream of the cylindrical grooves, this is due to the sudden section change.

This recirculation attributes to the braking of the flow, which means a long stay time for the fluid to pick up more calories from the lower wall (hot bed). The same thing is remarked from the Figure 9 that illustrates the velocity vectors around the triangular cavities. Hence, a strong recirculation of the flow is remarked around the triangular cavity more important than that of the cylindrical grooves.

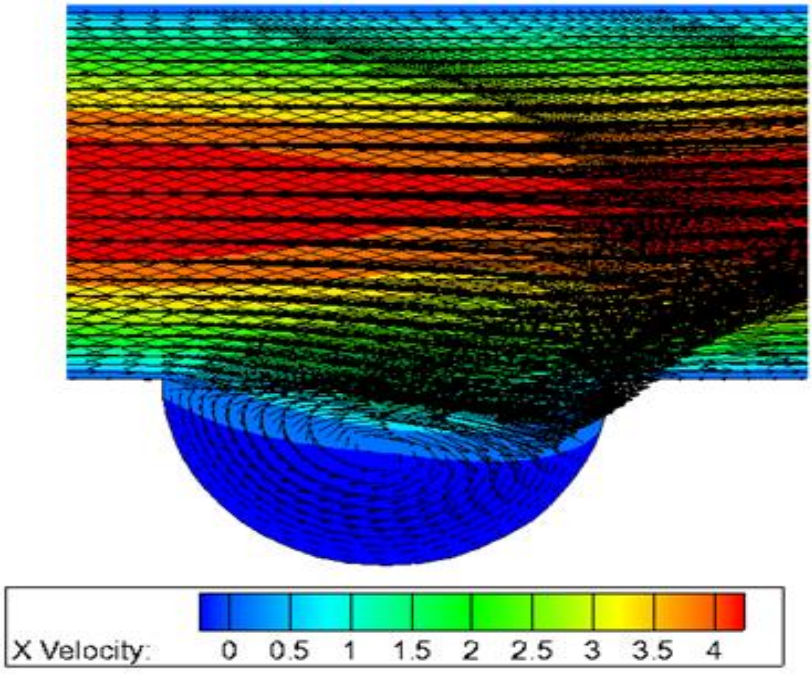

Figure 8. Velocity vectors around the cylindrical groove.

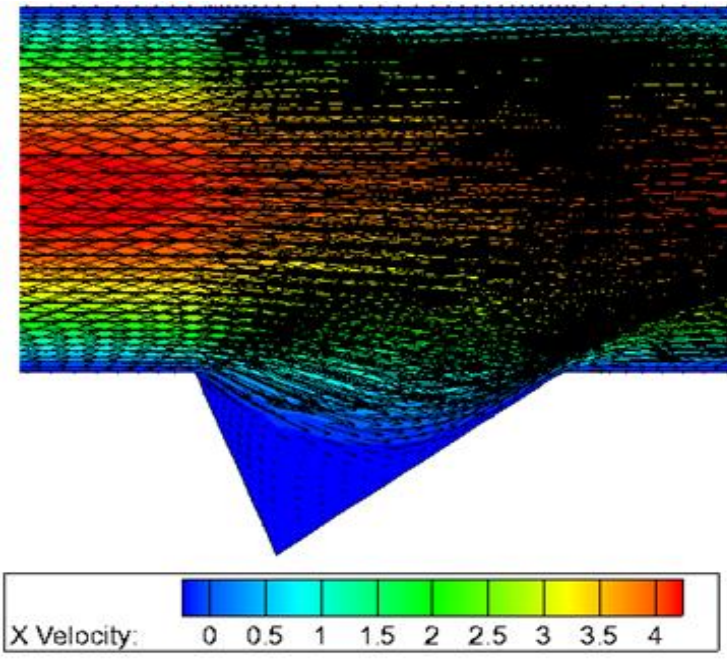

Figure 9. Velocity vectors around the triangular groove.

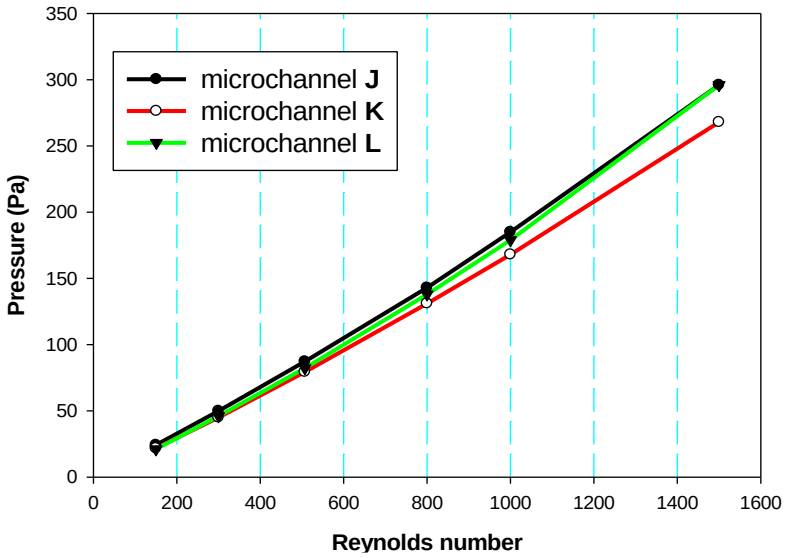

Figure 10. Pressure drop as a function of Reynolds number

The Figure 10 shows a linear relationship between pressure drop and Reynolds number, in reference to the simple microchannel, the proposed microchannels has the lower pressure drop for Reynolds number ranging 150-1000, especially for the microchannel with cylindrical grooves where the pressure drop decreases. For Re>= 1000, the pressure drop in the microchannel with triangular cavities is nearly similar to that one of smooth microchannel. It is noticed that with Reynolds number increasing 300-1500, the pressure drop increase with 320%.

The Figure 11 presents the behavior of average friction coefficient with Reynolds number ranging, the figure showed that the product f.Re increase with Reynolds number especially when Reynolds number pass 500.The addition of cross section has ameliorated the average friction coefficient, especially for triangular reentrant cavities.

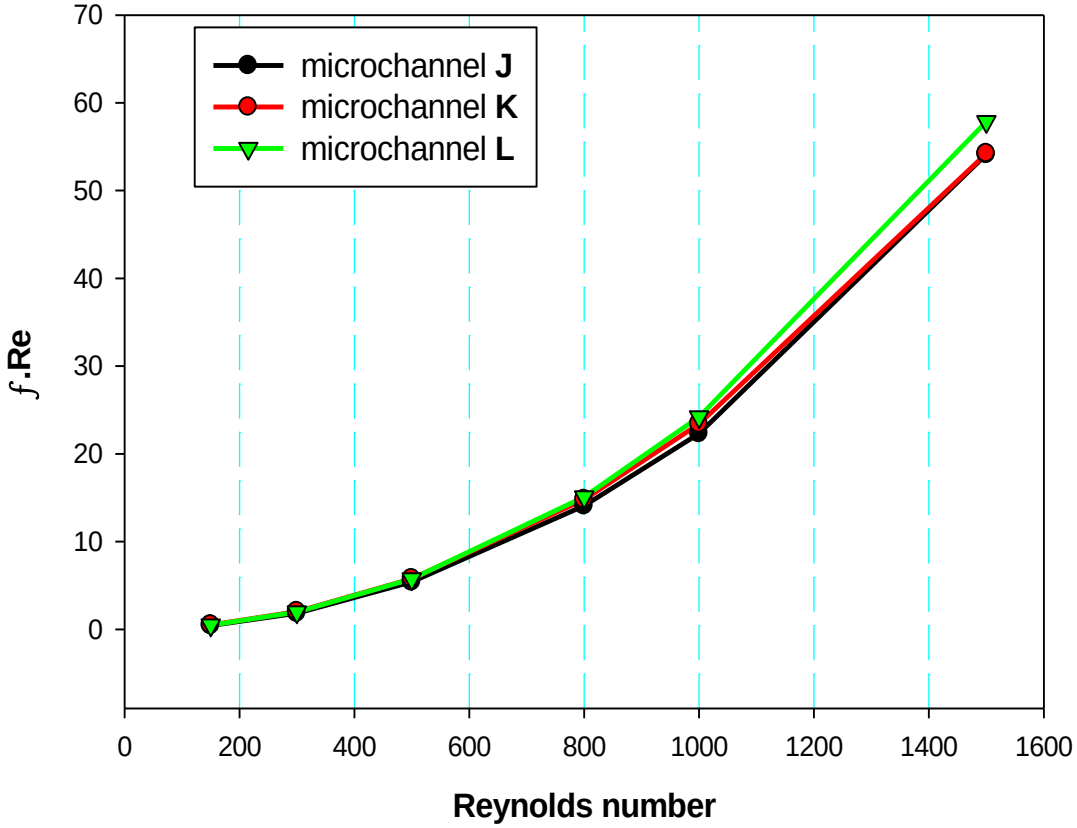

Figure 11. f.Re versus Reynolds number.

Heat transfer

In the figure 12, we presented the temperature contour; it showed that the higher temperatures are remarked in the lower wall, which is the heat source, the added sections have enhanced the high temperature layer, which expand when the Reynolds number increase.

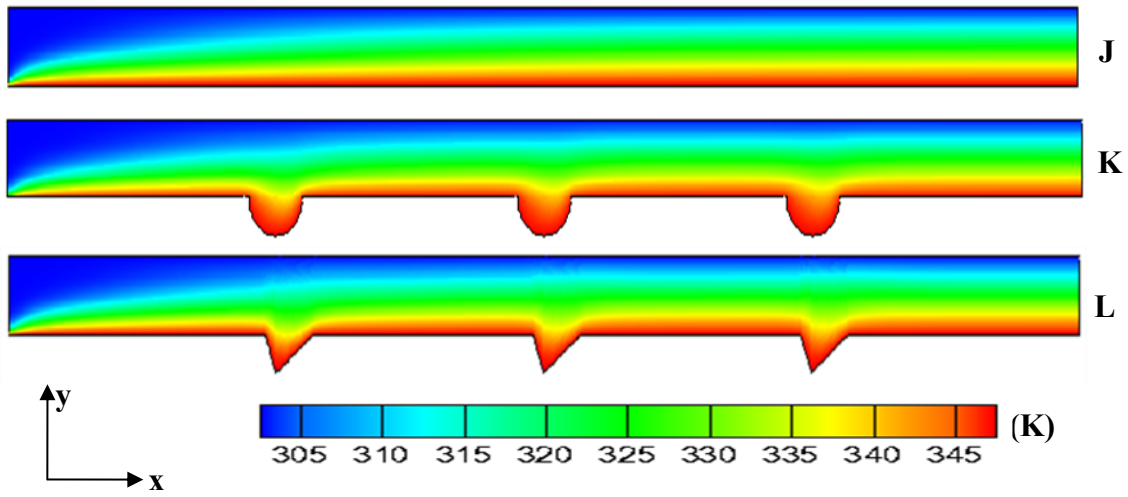

Figure 12. Temperature distribution in microchannels at Re=500.

The figure 13 presents the local Nusselt number behavior with the length of microchannel at the lower wall, it showed that the local Nusselt number decrease gradually from the inlet to the outlet, and it reached every added section.

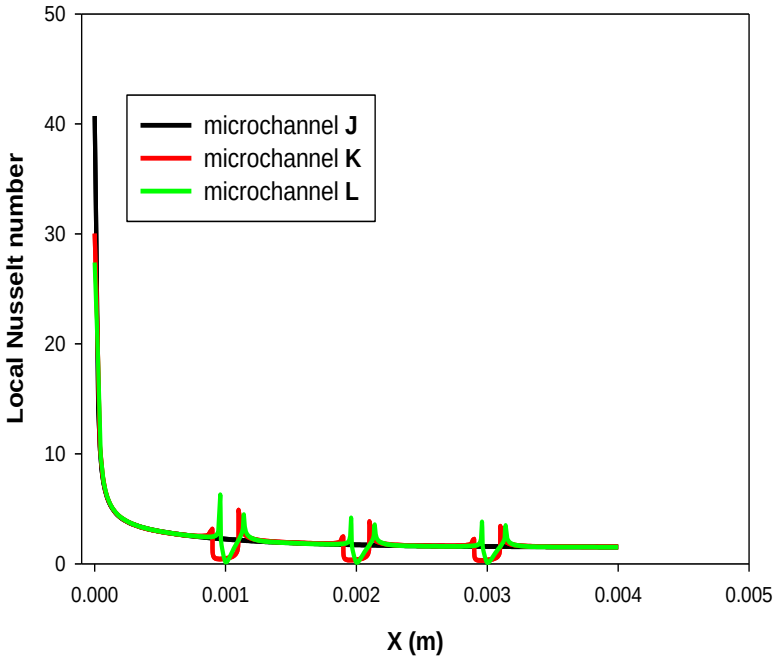

Figure 13. Local Nusselt number at the lower wall at Re=500.

The effect of the periodic expansion-constriction cross section on the local Nusselt number is illustrated in the figure 14, where the added sections have ameliorated the local Nusselt number from the downstream of the cylindrical grooves (microchannel K), and from the upstream for the triangular reentrant cavities (microchannel

L). However, inside the added sections the heat transfer is lower than that one of the microchannel without the added sections.

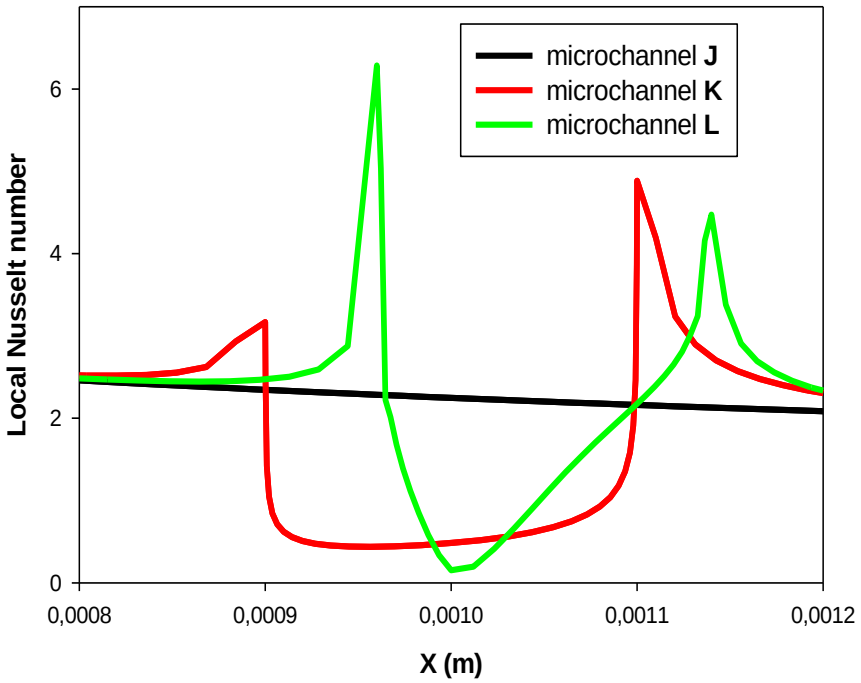

Figure 14. Local Nusselt number according to the lower wall at Re=500.

The average Nusselt number is studied as a function of Reynolds number in figure 15; it showed that the Nusselt number increase with the Reynolds number, and that the two newly microchannels give an average Nusselt number higher than that of the simple microchannel (J).

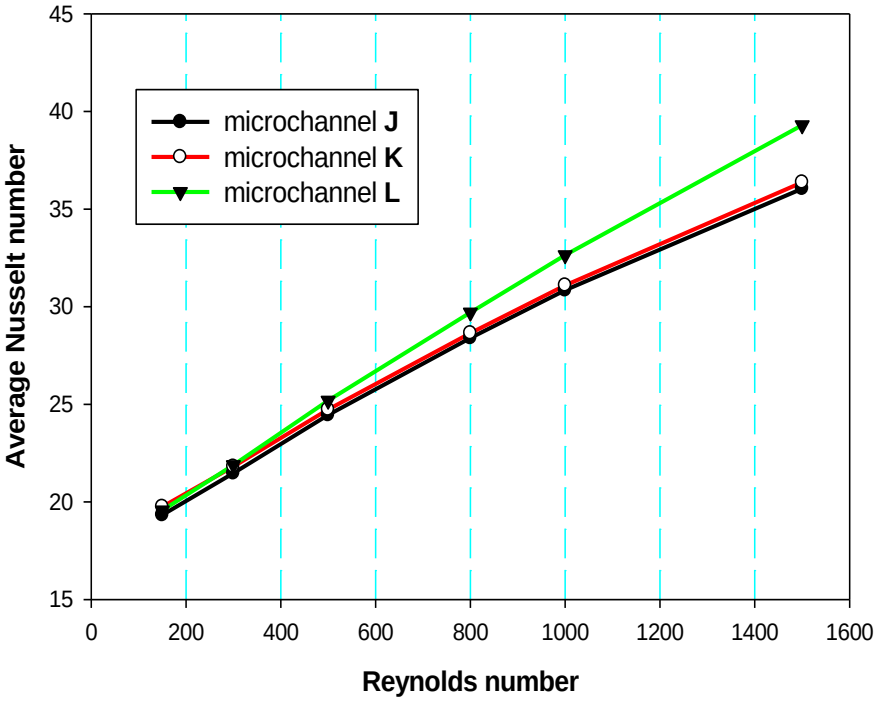

Figure 15. Average Nusselt number as a function of Reynolds number.

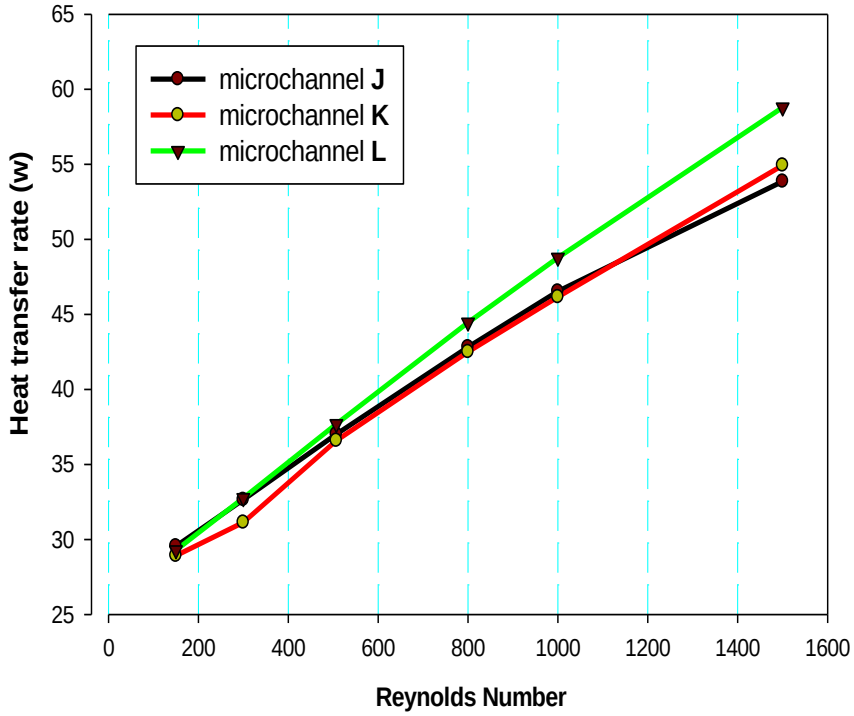

Figure 16. Heat transfer rate versus Reynolds number.

Heat transfer efficiency of microchannels heat sinks

In order to compare between the microchannels, the figure17 illustrates the heat transfer efficiency as a function of Reynolds number, it showed that microchannels with periodic expansion-constriction cross-section have a higher efficiency than that of the simple microchannel, and the microchannel with triangular reentrant cavities is the best microchannel in reference to his efficiency than other microchannels.

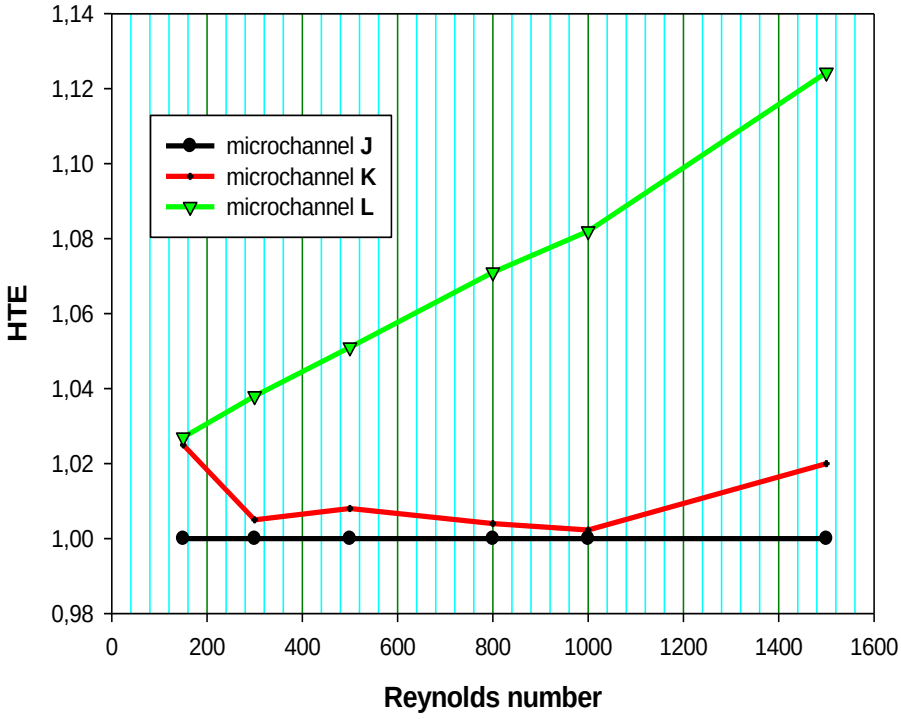

Figure 17. Heat Transfer Efficiency as a function of Reynolds number.

CONCLUSION

A numerical investigation has been executed to study a laminar, forced convective flow in microchannels with periodic expansion-constriction cross-section. In order to study the effect of those added cross-sections on the dynamic and thermal behavior of water flow used for cooling systems.

The governing partial differential equations were solved using the finite volume formulation along with the SIMPLE algorithm (Semi-Implicit Method for Pressure-Linked Equations). The profiles and the distribution of axial velocities show a stagnation in proximity with added cross-sections, the pressure drop is lower in microchannels with expansion-constriction cross-section in reference to the simple microchannel; even the fiction coefficient was enhanced.

The influence of the added sections on the thermal parameters is determinant: the Nusselt number is increasing with the rise of Reynolds number for all microchannels, it is worth noting that heat transfer rate is enhanced remarkably by the periodic expansion-cross section, as showed the local Nusselt number. Microchannels with cross section changing present small fluctuations corresponding to its Nusselt numbers, which is much higher at the entrance of microchannels region. It decreases in expansion and it increases in constriction cross-section, this thermal amelioration conducts to obtain a good heat transfer efficiency for microchannels. These results show that microchannels with triangular cavities are more efficient than microchannels with cylindrical grooves.

In this study, we have succeeded to ameliorate the heat transfer using a convective forced flow in microchannels heat sinks for electronic cooling systems.

NOMENCLATURE

Cp	Specific heat at constant pressure, (J/kg K)
Dh	Hydraulic diameter of microchannels, (m)
f	Friction factor
h	Convective heat exchange coefficient, (w/m2.K)
J	Rectangular microchannel
K	Microchannel with dimples
L	Microchannel with triangular cavities
m	Mass flow rate of fluid (kg/s)
Nu	Local Nusselt number
$\overline{(Nu)}$	Average Nusselt number
Q	Heat transfer rate, (w)
P	Pressure, (Pa)
Re	Reynolds number
T	Temperature, (K)
Ui	Velocity inlet, (m/s)
u,v	Fluid velocity in the x, y directions, (m/s)
x,y	Cartesian coordinates, (m)
ρ	Density of water, (kg/m3)
λ	Thermal conductivity, (w/m.K)
μ	Dynamic viscosity, (kg/m.s)
Δp	Pressure drop
f	fluid
i	inlet
J	Rectangular microchannel
m	mean
mic	Microchannel

REFERENCES

[1] Berlin, A. A., & Gabriel, K. J. (1997). Distributed MEMS: New challenges for computation. IEEE Computational Science and Engineering, 4(1), 12-16.

[2] Tuckerman, D. B., & Pease, R. F. W. (1981). High-performance heat sinking for VLSI. IEEE Electron device letters, 2(5), 126-129.

[3] Samalam, V. K. (1989). Convective heat transfer in microchannels. Journal of Electronic Materials, 18(5), 611-617.

[4] Peng, X. F., Peterson, G. P., & Wang, B. X. (1994). Heat transfer characteristics of water flowing through microchannels. Experimental Heat Transfer An International Journal, 7(4), 265-283.

[5] Peng, X. F., & Peterson, G. P. (1996). Convective heat transfer and flow friction for water flow in microchannel structures. International journal of heat and mass transfer, 39(12), 2599-2608.

[6] Li, J., & Peterson, G. P. (2005). Boiling nucleation and two-phase flow patterns in forced liquid flow in microchannels. International journal of heat and mass transfer, 48(23-24), 4797-4810.

[7] Margot, X., Hoyas, S., Gil, A., & Patouna, S. T. A. V. R. O. U. L. A. (2012). Numerical modelling of cavitation: validation and parametric studies. Engineering Applications of Computational Fluid Mechanics, 6(1), 15-24.

[8] Sheikholeslami, M., Vajravelu, K., & Rashidi, M. M. (2016). Forced convection heat transfer in a semi annulus under the influence of a variable magnetic field. International Journal of Heat and Mass Transfer, 92, 339-348.

[9] Sheikholeslami, M., Rashidi, M. M., & Ganji, D. D. (2015). Effect of non-uniform magnetic field on forced convection heat transfer of Fe3O4–water nanofluid. Computer Methods in Applied Mechanics and Engineering, 294, 299-312.

[10] Sheikholeslami, M., Rashidi, M. M., & Ganji, D. D. (2015). Effect of non-uniform magnetic field on forced convection heat transfer of Fe3O4–water nanofluid. Computer Methods in Applied Mechanics and Engineering, 294, 299-312.

[11] Farhanieh, B., Herman, Č., & Sundén, B. (1993). Numerical and experimental analysis of laminar fluid flow and forced convection heat transfer in a grooved duct. International journal of heat and mass transfer, 36(6), 1609-1617.

[12] Qu, W., & Mudawar, I. (2002). Analysis of three-dimensional heat transfer in micro-channel heat sinks. International Journal of heat and mass transfer, 45(19), 3973-3985.

[13] Chai, L., Xia, G., Zhou, M., Li, J., & Qi, J. (2013). Optimum thermal design of interrupted microchannel heat sink with rectangular ribs in the transverse microchambers. Applied Thermal Engineering, 51(1-2), 880-889.

[14] Weilin, Q., Mala, G. M., & Dongqing, L. (2000). Pressure-driven water flows in trapezoidal silicon microchannels. International journal of heat and mass transfer, 43(3), 353-364..

[15] Ghaedamini, H., Lee, P. S., & Teo, C. J. (2013). Developing forced convection in converging–diverging microchannels. International Journal of Heat and Mass Transfer, 65, 491-499.

[16] Gong, L., Kota, K., Tao, W., & Joshi, Y. (2011). Parametric numerical study of flow and heat transfer in microchannels with wavy walls. Journal of Heat Transfer, 133(5), 051702.

[17] Zheng, Z., Fletcher, D. F., & Haynes, B. S. (2013). Laminar heat transfer simulations for periodic zigzag semicircular channels: chaotic advection and geometric effects. International Journal of Heat and Mass Transfer, 62, 391-401.

[18] Liu, Y., Cui, J., Jiang, Y. X., & Li, W. Z. (2011). A numerical study on heat transfer performance of microchannels with different surface microstructures. Applied Thermal Engineering, 31(5), 921-931.

[19] Xia, G., Chai, L., Zhou, M., & Wang, H. (2011). Effects of structural parameters on fluid flow and heat transfer in a microchannel with aligned fan-shaped reentrant cavities. International Journal of Thermal Sciences, 50(3), 411-419.

[20] Xia, G., Chai, L., Wang, H., Zhou, M., & Cui, Z. (2011). Optimum thermal design of microchannel heat sink with triangular reentrant cavities. Applied Thermal Engineering, 31(6-7), 1208-1219.

[21] Chai, L. Xia,G.D. Wang,L. Zhou, M.Z and Cui, Z.Z., Heat transfer enhancement in microchannel heat sinks with periodic expansion–constriction cross-sections, Int. J. Heat Mass Trans., 2013 62,741–751.

[22] Gururatana, S. (2012). Numerical simulation of micro-channel heat sink with dimpled surfaces. American Journal of Applied Sciences, 9(3), 399.

[23] Dehghan, M., Daneshipour, M., Valipour, M. S., Rafee, R., & Saedodin, S. (2015). Enhancing heat transfer in microchannel heat sinks using converging flow passages. Energy Conversion and Management, 92, 244-250.

[24]Patankar, S.V., (1980). Numerical Heat Transfer and Fluid Flow. 1st Edn, Hemisphere Publication Corporation, Washington: ISBN: 0070487405.

[25] Grigull, U., & Tratz, H. (1965). Thermischer einlauf in ausgebildeter laminarer rohrströmung. International Journal of Heat and Mass Transfer, 8(5), 669-678.